Effect of Alkyl Substituents and Ring Size on Alkoxy Radical Cleavage Reactions

Sarah Wilsey,[†] Paul Dowd,[‡] and K. N. Houk*,[†]

Department of Chemistry and Biochemistry, University of California, Los Angeles, California, 90095-1569, and Department of Chemistry, University of Pittsburgh, Pittsburgh, Pennsylvania 15260

Received April 20, 1999

The α-cleavage ring-opening reactions of a series of acyclic and cyclic alkoxy radicals are examined computationally with CASSCF/6-31G*, UHF/6-31G*, and UB3LYP/6-31G* methods, to explain the anomalous results obtained by Zhang and Dowd (*Tetrahedron* **1993**, *49*, 1965): tricyclic alkoxy radicals were found to cleave to give the less-stable products in several cases; even allylic stabilization of the radical formed by cleavage does not influence the direction of cleavage. The source of this kinetic preference is identified as arising from two factors: (i) through-bond interactions significantly slow the rate of bond cleavage in fused four-membered rings relative to exocyclic cleavage of four-membered rings, and (ii) allylic stabilization is not effective in the early transition state of alkoxy radical cleavage in these strained systems. The relationship between activation energies of cleavage and the energy of the reaction is explored for a variety of cyclic and acyclic alkoxy radicals. Benson's observation that the ease of cleavage is related to both the heat of reaction and the ionization potential of the radical formed (*Int. J. Chem. Kinet.* **1981**, *13*, 833) is confirmed and extended to more examples.

Introduction

Alkoxy radicals normally cleave to give a ketone (or aldehyde) and the most stable possible alkyl radical.[1] Much work was carried out in the late 1950s and early 1960s determining the factors that control the competitive rates of fission of substituent groups from alkoxy radicals. These reactions are usually governed by the thermodynamic stability of the products formed,[1,2] although solvent effects and ring strain also contribute.[2] Choo and Benson reevaluated kinetic data on alkoxy radical cleavages and the reverse reactions and found that the activation energy of addition depends not only on the heat of reaction, but also on the ionization potential (IP) of the radical which adds to the carbonyl group.[3] $E_a = 2.1[\mathrm{IP(R)}] - 6.2 - 0.58[\Delta H]$, for the addition reaction.

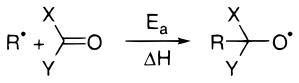

For the cleavage reaction (reverse of above), $E_a^{\mathrm{cleavage}} = 2.1[\mathrm{IP(R)}] - 6.2 + 1.58[\Delta H^{\mathrm{cleavage}}]$.

Bond cleavage leading to the formation of an allylic radical is expected to be particularly favorable due to the stability of the radical formed and its relatively low IP. However, Zhang and Dowd discovered a number of examples where cleavage of an alkoxy radical with ring-opening does *not* give the thermodynamically more stable product.[4] We have studied alkoxy cleavage reactions with quantum mechanical calculations at several different levels (CASSCF, UHF, and UB3LYP) and have discovered an explanation for the origins of these phenomena.

Background

Radical cyclizations involving the addition of carbon radicals to carbonyl groups leading to oxy radicals were proposed by Dowd et al. as a synthetic route to the diastereomeric natural products (±)-trichodiene (**1**) and (±)-bazzanene (**2**), starting from bicyclo[4.2.0]octenones.[4]

1 **2**

It was expected that an alkoxy radical intermediate, **3** (Scheme 1), would be formed, which could undergo cyclobutane ring cleavage to form an allylic radical (bond **a** cleavage), a precursor of the natural products.

However, contrary to expectation, the allylic cleavage process gave the minor product **6**; the seven-membered ring product **5** (corresponding to bond **b** cleavage) was formed in 80% yield.

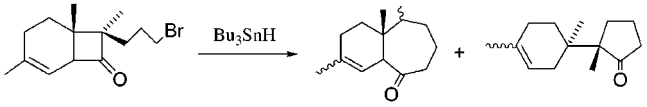

4 **5** 80% **6** 11%

Both bond cleavages result in the relief of cyclobutane

[†] University of California, Los Angeles.

[‡] University of Pittsburgh. Deceased Nov 21, 1996.

(1) (a) Kochi, J. K. *J. Am. Chem. Soc.* **1962**, *84*, 1193. (b) Kochi, J. K. *Free Radicals*; Kochi, J. K., Ed.; Wiley-Interscience: New York, 1973; Vol. 2, p 665. (c) Gray, P.; Williams, A. *Chem. Rev.* **1959**, *59*, 239.

(2) (a) Bacha, J. D.; Kochi, J. K. *J. Org. Chem.* **1965**, *30*, 3272. (b) Greene, F. D.; Savitz, M. L.; Osterholtz, F. D.; Lau, H. H.; Smith, W. N.; Zanet, P. M. *J. Org. Chem.* **1963**, *28*, 55. (c) Walling, C.; Wagner, P. J. *J. Am. Chem. Soc.* **1963**, *85*, 2333. (d) Walling, C.; Padwa, A. *J. Am. Chem. Soc.* **1963**, *85*, 1593.

(3) Choo, K. Y.; Benson, S. W. *Int. J. Chem. Kinet.* **1981**, *13*, 833.

(4) Zhang, W., Dowd, P. *Tetrahedron* **1993**, *49*, 1965.

10.1021/jo990652+ CCC: $18.00
Published on Web 11/26/1999

Scheme 1

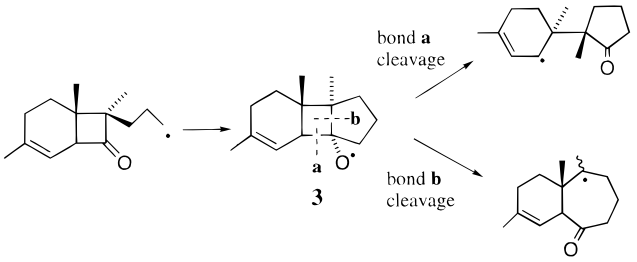

ring strain, but the allylic bond was expected to be the main site of bond cleavage, as this gives the more stable radical product. The reaction was also investigated with a substrate lacking the C=C double bond. Surprisingly, treatment of **7** with Bu_3SnH gave *more* cleavage (22%) of bond **a** to form the cyclohexyl radical.

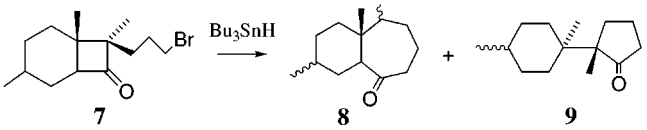

The effect of removing the angular methyl group was also examined: ring-opening of the intermediate formed from **10** yields a secondary radical in competition with allylic cleavage.

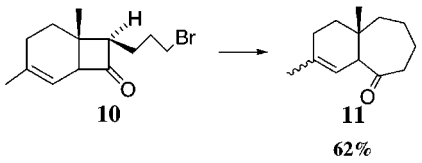

Remarkably, the methyl group effect is also contrary to expectation as 62% of **11** was observed, but no allylic product was formed at all. When the double bond was removed, 14% of **14** was observed.

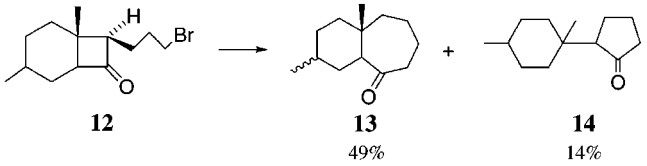

Here we investigate the factors contributing to the relative efficiencies of the two types of ring cleavage to determine why formation of an allylic radical should be disfavored relative to the formation of the seven-membered ring product. A series of primary (eqs **A**−**E**; radicals **15**−**19**), secondary (**F**−**J**; **20**−**24**), and tertiary (**K**−**O**; **25**−**29**) acyclic alkoxy radicals (see Figures 1−3) were investigated to provide baseline comparison. Bond cleavage in a number of different cyclic systems (**P**−**W**) (shown in Figures 4−6) will be discussed. These include the monocyclic radicals cyclopropoxy (**30**), cyclobutoxy (**33**), cyclopentoxy (**36**), and cyclohexoxy (**39**) and, as models for systems **4** and **7**, the bicyclic and tricyclic systems **T**, **U**, **V**, and **W**. Compound **42** has fused cyclobutane and cyclopentane rings, **47** has an additional vinyl group, and structures **52** and **57** contain fused cyclohexane and cyclohexene rings, respectively.

In each case, the reactant alkoxy radical, transition structures, and product radicals were optimized using

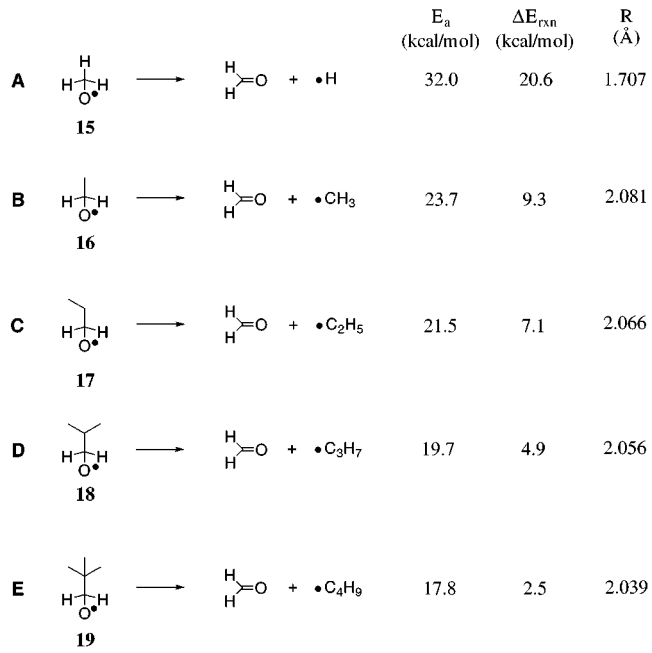

Figure 1. Primary acyclic alkoxy radical systems with activation energies, energies of reaction (kcal/mol), and breaking CC bond distance in the transition state (*R*) computed at the CASSCF/6-31G* level.

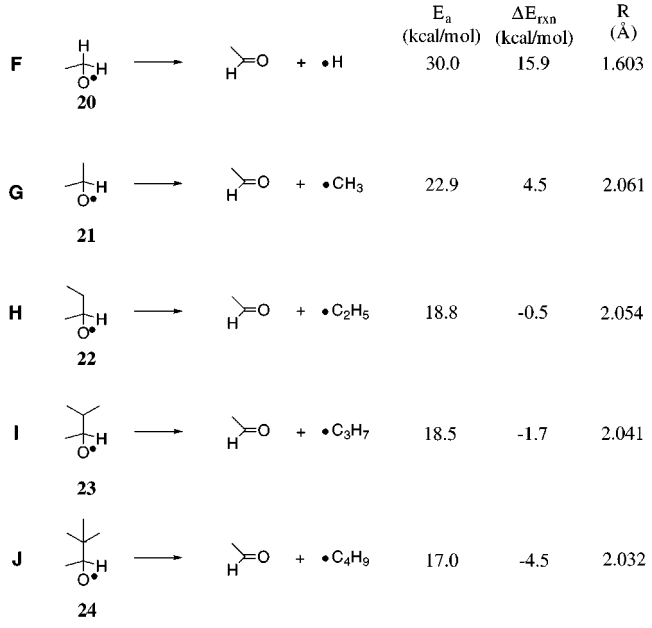

Figure 2. Secondary acyclic alkoxy radical systems computed at the CASSCF/6-31G* level. Definitions as in Figure 1.

CASSCF and the 6-31G* basis set. The transition structures for systems **V** and **W** were also optimized using UHF/6-31G* and UB3LYP/6-31G* methods. Finally, the transition structures for the six different methyl-substituted systems **V1**, **V2**, **V3**, **W1**, **W2**, and **W3**, shown in Scheme 2, were also located at a lower level of theory (CASSCF/4-31G//CASSCF/STO-3G), to see if the methyl groups have a significant effect on the barrier heights.

Computational Procedure

The alkoxy radical reactants, product alkyl radicals, and transition structures were fully optimized for the systems **A**−**W** at the CASSCF/6-31G* level using the code implemented

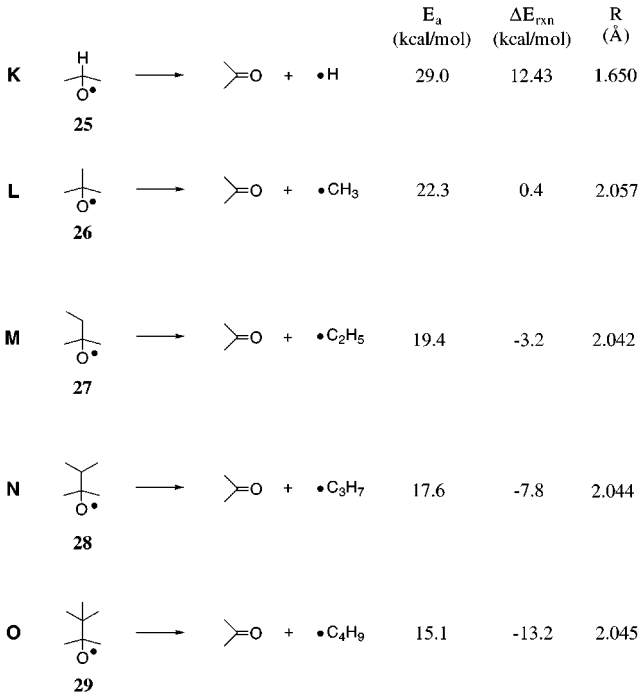

Figure 3. Tertiary acyclic alkoxy radical systems computed at the CASSCF/6-31G* level. Definitions as in Figure 1.

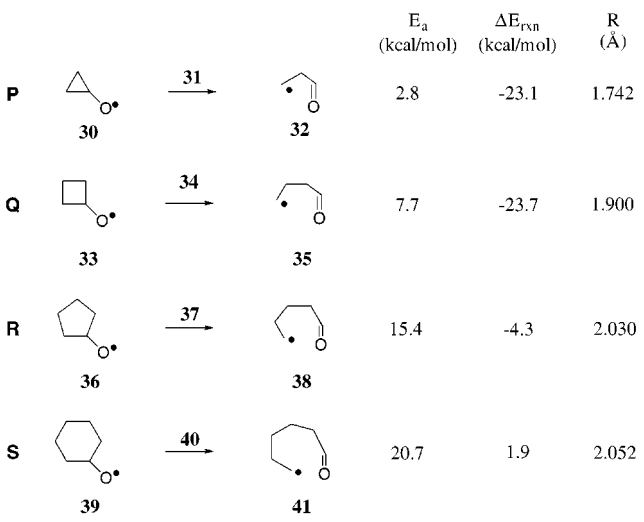

Figure 4. Monocyclic systems computed at the CASSCF/6-31G* level. Definitions as in Figure 1.

in GAUSSIAN 94.[5] For the systems **V1**, **V2**, **V3**, **W1**, **W2**, and **W3**, the geometries were optimized at the STO-3G level, and then single points were computed using the 4-31G basis set. The active space chosen for the acyclic systems **A**−**O** and the monocyclic systems **P**−**S** included the σ orbitals in the bond that is cleaved and the singly occupied nonbonding molecular orbital (SOMO) on the oxygen atom, that is, three electrons in three orbitals. For the bicyclic and tricyclic systems **T**−**W**, a CAS (5,5) active space was used. The active space for each alkoxy radical contained the σ orbitals involved in the two

(5) GAUSSIAN 94 (Revision B2): Frisch, M. J.; Trucks, G. W.; Schlegel, H. B.; Gill, P. M. W.; Johnson, B. G.; Robb, M. A.; Cheeseman, J. R.; Keith, T. A.; Petersson, G. A.; Montgomery, J. A.; Raghavachari, K.; Al-Laham, M. A.; Zakrzewski, V. G.; Ortiz, J. V.; Foresman, J. B.; Cioslowski, J.; Stefanov, B. B.; Nanayakkara, A.; Challacombe, M.; Peng, C. Y.; Ayala, P. Y.; Chen, W.; Wong, M. W.; Andres, J. L.; Replogle, E. S.; Gomperts, R.; Martin, R. L.; Fox, D. J.; Binkley, J. S.; Defrees, D. J.; Baker, J.; Stewart, J. P.; Head-Gordon, M.; Gonzalez, C.; Pople, J. A., Gaussian, Inc., Pittsburgh, PA, 1995.

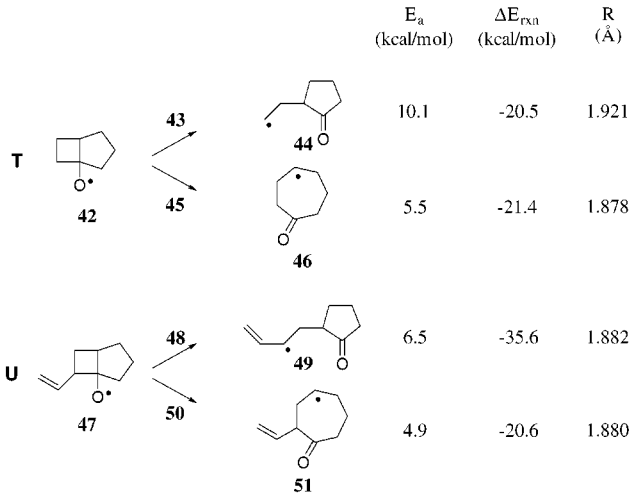

Figure 5. Bicyclic systems computed at the CASSCF/6-31G* level. Definitions as in Figure 1.

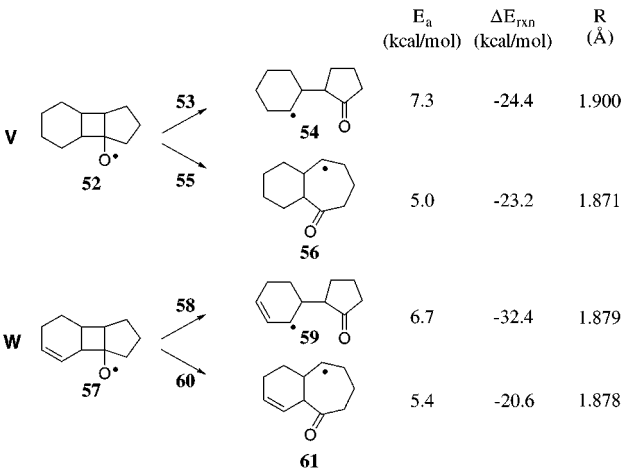

Figure 6. Tricyclic systems computed at the CASSCF/6-31G* level. Definitions as in Figure 1.

bonds (**a** and **b** in Scheme 1) that can be cleaved and the singly occupied oxygen nonbonding orbital. These orbitals eventually evolve into the C=O π and π^* orbitals and the SOMO on the alkyl fragment in the products. For the alkene systems **U**, **W**, **W1**, **W2**, and **W3**, the π and π^* orbitals of the C=C bond were also included, making a CAS (7,7) active space in total. In each case, the lowest energy doublet state was studied.

Energies were not zero point energy corrected as frequency calculations proved too expensive for the large systems **T**−**W**. In each case the activation energy quoted is the difference between the energies of the transition structure and the reactant molecule, while the reaction energy is the difference between the energies of the product molecules and those of the reactant molecules.

CASSCF energies are known to lack some dynamic correlation, and therefore activation energies tend to be overestimated. However, these errors are expected to be consistent such that the trends are not expected to be affected by this error. UHF also has a tendency to significantly overestimate activation energies, and the energies of radicals can also suffer from the effects of spin contamination. Density functional methods, in particular with the Becke3LYP functional, have been shown to give remarkably good activation energies in many systems, although there is still some speculation as to their ability to describe radical and biradical systems. Additionally we had problems converging the transition state for bond **a** cleavage in system **W** using this method.

Scheme 2

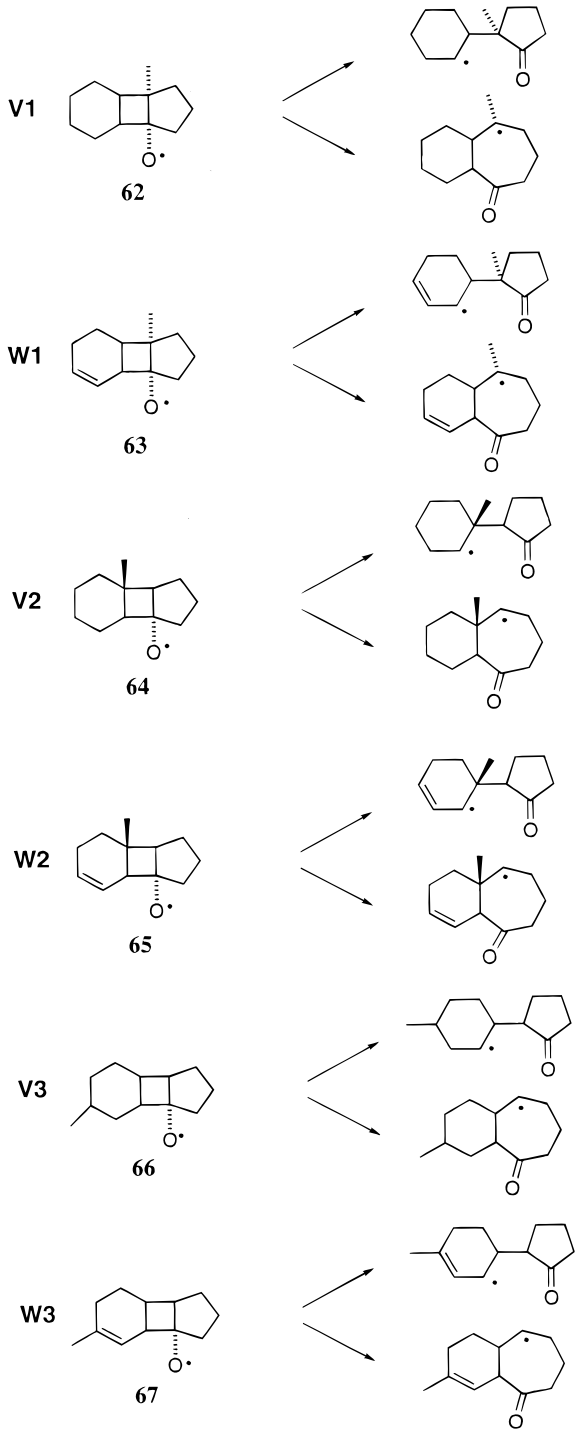

Results

(i) Acyclic Systems. Figures 1−3 show the activation energies and reaction energies computed at CASSCF/6-31G* for a series of primary (**15**−**19**), secondary (**20**−**24**), and tertiary (**25**−**29**) acyclic alkoxy radicals, respectively. In each the loss of a hydrogen, methyl, ethyl, isopropyl, and *tert*-butyl radical was examined. A number of experimental results are available or have been estimated by Benson.[3] The CASSCF results for the cleavage of single acyclic alkoxy radicals generally give energies of reaction which are 4−5 kcal/mol more exothermic than those found by Benson, while the computed activation energies are 4−8 kcal/mol above those estimated by Benson from experimental data.[3] The latter is expected due to the neglect of dynamic correlation energy in the CASSCF calculations.

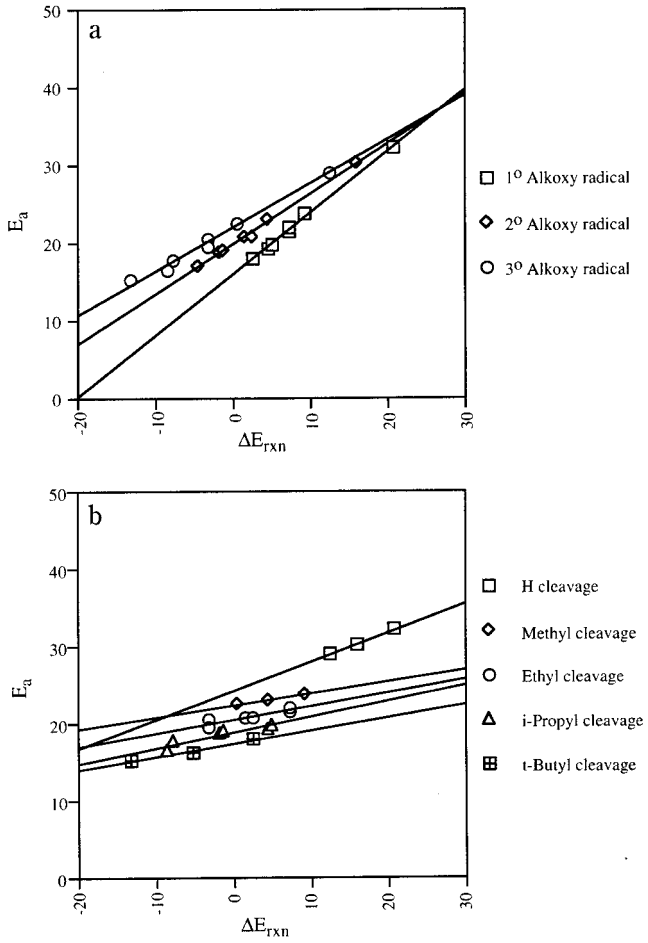

Figure 7. Graph of activation energy E_a versus the energy of reaction ΔE_{rxn} for the acyclic alkoxy radical systems computed at the CASSCF/6-31G* level. (a) The three lines represent the lines of best fit for the primary, secondary, and tertiary radical systems, respectively. (b) The lines are drawn through points involving the same radical fragment.

Figure 7 shows two different plots of activation energy (E_a) against the energy of reaction (ΔE_{rxn}) for these acyclic systems. The graph in Figure 7a shows three distinct lines of best fit corresponding to the primary, secondary, and tertiary alkoxy radicals. The correlation coefficients, r^2, are greater than 0.98 in each case, indicating a linear relationship between E_a and ΔE_{rxn} for each type of radical. As the leaving group becomes more substituted, both the transition state and the products are stabilized. The straight lines indicate that the fraction of change in product stabilization that shows up in the transition state (equal to the slope of the line) is large and constant for each type of radical; these fractions are 0.79, 0.65, and 0.56 for the primary, secondary, and tertiary radicals, respectively. Furthermore, for a primary alkoxy radical, the activation energy for cleavage is lower than that for a secondary or tertiary cleavage of the same endothermicity.

In Figure 7b, lines are drawn through systems with the same leaving alkyl radical, as in the earlier Choo−Benson treatment.[3] These lines have slopes between 0.16 and 0.21 for all leaving groups except hydrogen, where the slope is 0.38. Benson showed earlier that, for a given

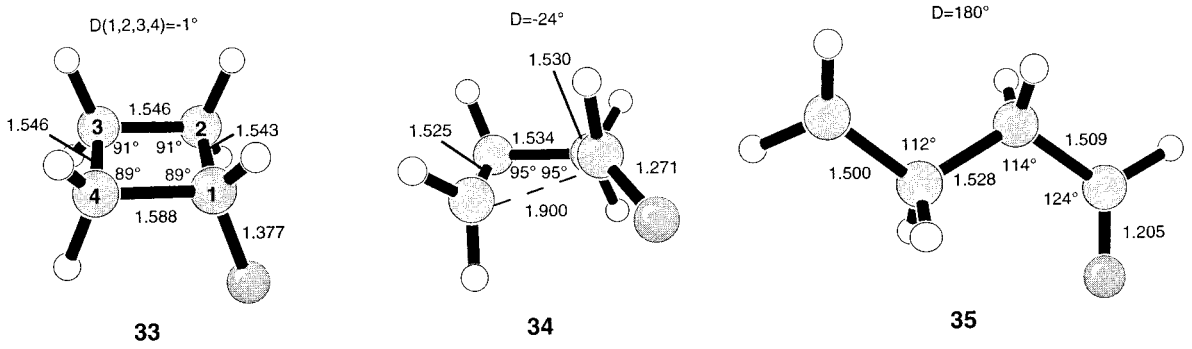

Figure 8. CASSCF/6-31G*-optimized cyclobutoxy geometries—cyclobutoxy radical (**33**), cleavage transition structure **34**, and anti cleavage product **35**.

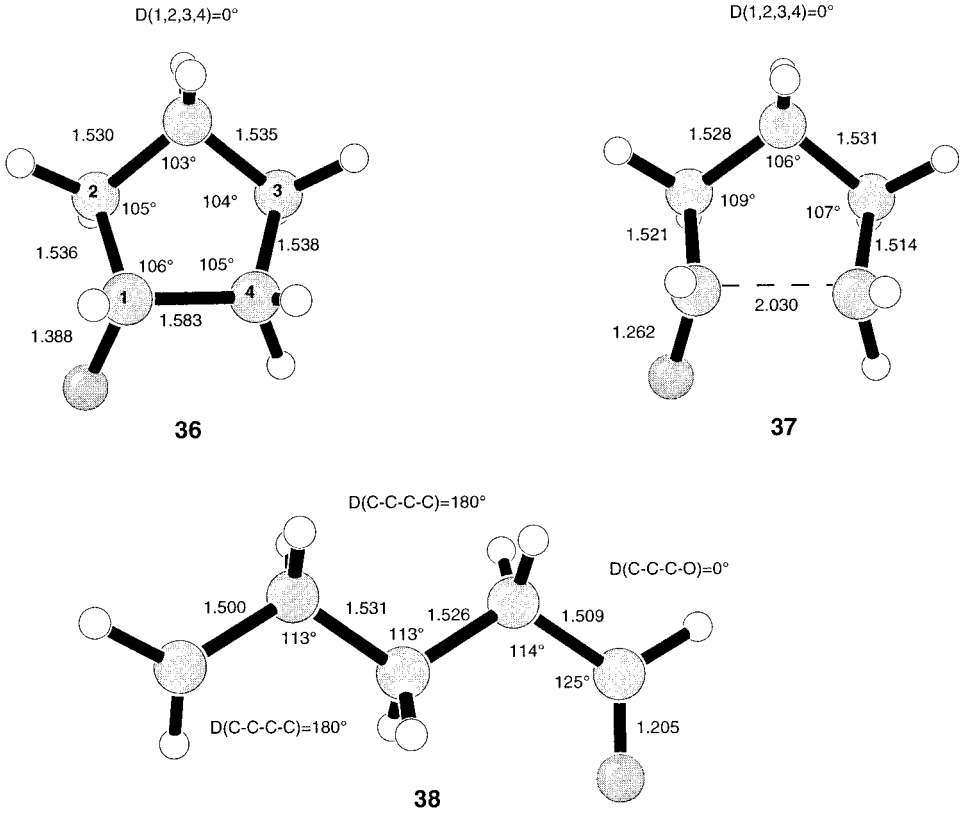

Figure 9. CASSCF/6-31G*-optimized cyclopentoxy geometries—cyclopentoxy radical (**36**), cleavage transition structure **37**, and anti cleavage product **38**.

heat of reaction, loss of radicals with a low IP occurs with a lower E_a than formation of radicals with a higher IP, consistent with a polarized transition state of the form

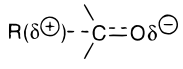

(ii) Cyclic Systems. Figure 4 shows the activation energies and reaction energies computed at the CASSCF/6-31G* level for the monocyclic systems **P**, **Q**, **R**, and **S**. Also shown are the lengths of the breaking bonds (*R*) in the transition states. The cleavage of the cyclopropoxy radical **30** to form the product radical **32** is highly exothermic. This is consistent with the early transition state **31**, where the C−C bond-breaking distance is only 1.74 Å. The geometries are not shown but can be obtained as Supporting Information.

Figure 8 shows the optimized geometries of the cyclobutoxy radical **33**, transition structure **34**, and ring cleavage product **35**. Surprisingly, the exothermicity of cyclobutoxy cleavage is slightly greater than that of the cyclopropoxy system (23.7 kcal/mol versus 23.1 kcal/mol). However, the barrier for cyclobutoxy cleavage is 5 kcal/mol higher than for cyclopropoxy cleavage. These results are reminiscent of those observed in cycloalkylcarbinyl systems where the activation energy for cleavage of the cyclobutylcarbinyl radical is 6.5−7.5 kcal/mol higher than for the cyclopropylcarbinyl system.[6] The cyclobutoxy transition structure has a longer bond-breaking distance (1.90 Å) than that of the cyclopropoxy system, indicating a later transition state. The lowest energy transition structure has the oxygen atom pseudoequatorial when the bond breaks. The preference for pseudoequatorial versus pseudoaxial cleavage is reminiscent of the stereoselectivity of cyclobutene ring-opening reactions, where

(6) Beckwith, A. L. J.; Moad, G. *J. Chem. Soc., Perkin Trans. 2* **1980**, 1083.

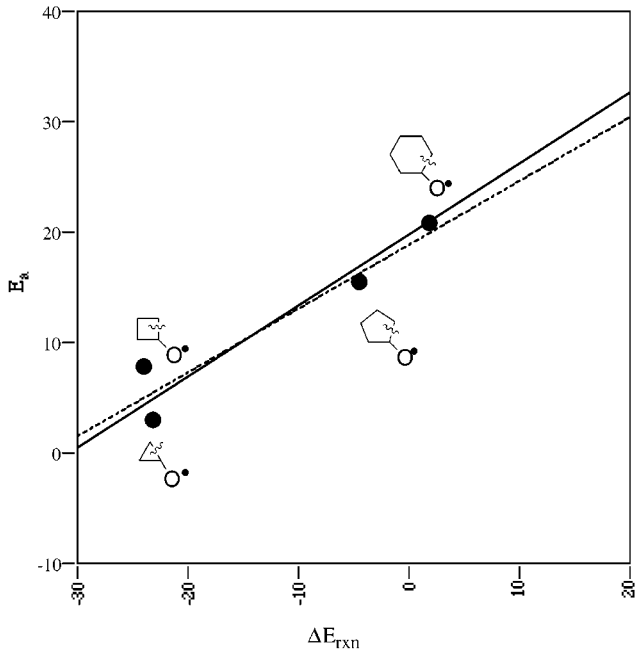

Figure 10. Graph of activation energy E_a versus the energy of reaction ΔE_{rxn} for the monocyclic systems computed at the CASSCF/6-31G* level.

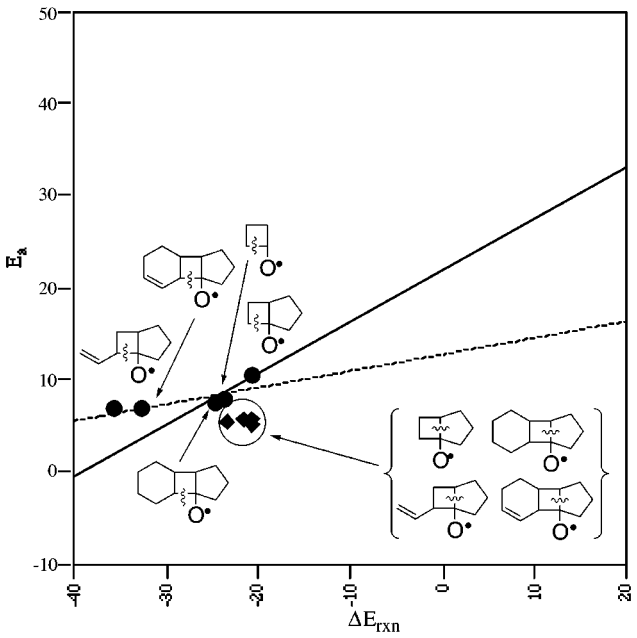

Figure 11. Graph of activation energy E_a versus the energy of reaction ΔE_{rxn} for the bicyclic and tricyclic systems computed at the CASSCF/6-31G* level.

oxygen and other donor substituents rotate outward as the C−C bond breaks.[7] Similarly, in cyclobutoxy, the oxygen rotates away from the breaking bond to avoid repulsive overlap of the oxygen lone pair and the σ orbitals of the breaking bond.

Ring cleavage of the cyclopentoxy radical **36** to form **38** (Figure 9), on the other hand, is a much less exothermic process due to the smaller degree of ring strain in the reactant radical. The reaction is only exothermic by 4.3 kcal/mol, and the activation barrier (15.4 kcal/mol) is much higher than for either the cyclopropoxy or cyclobutoxy system. This is consistent with the later transition state: the length of the breaking C−C bond in this case is 2.03 Å. The transition structure **37** involves pure C−C stretching, rather than twisting as in the cyclobutoxy case. In the lowest energy transition structure, four of the carbon atoms remain essentially in a plane; the fifth (the central carbon) lies above the plane, and the oxygen atom is trans to this central carbon. This transition structure has been computed previously by Beckwith et al. using the semiempirical AM1/UHF method.[8] They obtained a similar structure, but with a slightly shorter breaking bond length of 1.92 Å. Both the AM1 results and our CASSCF significantly overestimate the barrier to ring cleavage, which is estimated to be around 6 kcal/mol experimentally.[8,9]

Ring cleavage of the cyclohexoxy radical (**39**) is predicted to be endothermic by CASSCF/6-31G* calculations, as there is virtually no ring strain in the reactant radical. The activation energy is, accordingly, high. Again, the transition state corresponds mainly to a C−C stretch, and the bond-breaking distance is 2.05 Å. The geometries for the reactant **39**, transition structure **40**, and product radical **41** may be obtained as Supporting Information.

Beckwith also studied the reversible ring-opening of the cyclohexoxy radical both experimentally and theoretically and found that, while ring cleavage is slower than for the cyclopentyl radical (4.7×10^8 vs 1.1×10^7 for five- and six-membered rings, respectively), the rate of cyclization is actually higher for the 5-hexenyl radical (8.7×10^5 vs 1.0×10^6).[10] This is consistent with our results that predict that ring cleavage of the cyclohexoxy radical has a higher activation barrier, but is less exothermic, than that of the cyclopentoxy radical, even though experimentally the reaction is still predicted to be exothermic.

A plot of activation energy (E_a) against the energy of reaction (ΔE_{rxn}) for the monocyclic systems is shown in Figure 10. The line of best fit for these four systems is shown as a dashed line. These are secondary radicals, and therefore the line of best fit for the secondary acyclic radical systems is also shown in this graph as a solid line. The two lines are close to each other, showing that the secondary acyclic radicals are a reasonable model for the monocyclic systems. However, unlike the acyclic systems where the correlation coefficient $r^2 > 0.98$, there are significant deviations from both lines, especially for the cyclopropoxy and cyclobutoxy radicals such that $r^2 = 0.92$ in this case. The points for cyclopropoxy and cyclopentoxy lie below the line of best fit, while those corresponding to cyclobutoxy and cyclohexoxy lie above the line, the latter only slightly. The smaller deviations observed for the five- and six-membered systems indicate an effect that drops off with ring size.

It is often assumed that the activation energies for cleaving three-membered rings are lower than for cleaving four-membered rings due only to a difference in ring strain. However, the graph clearly indicates this is not the case. If this were true, then all the points would lie close to the line of best fit; cyclopropoxy and cyclobutoxy,

(7) Dolbier, W. R.; Koroniak, H.; Houk, K. N.; Sheu, C. M. *Acc. Chem. Res.* **1996**, *29*, 471.
(8) Beckwith, A. L. J.; Hay, B. P. *J. Am. Chem. Soc.* **1989**, *111*, 230.
(9) Walling, C.; Clark, R. T. *J. Am. Chem. Soc.* **1974**, *96*, 4530.
(10) Beckwith, A. L. J.; Hay, B. P. *J. Am. Chem. Soc.* **1989**, *111*, 2674.

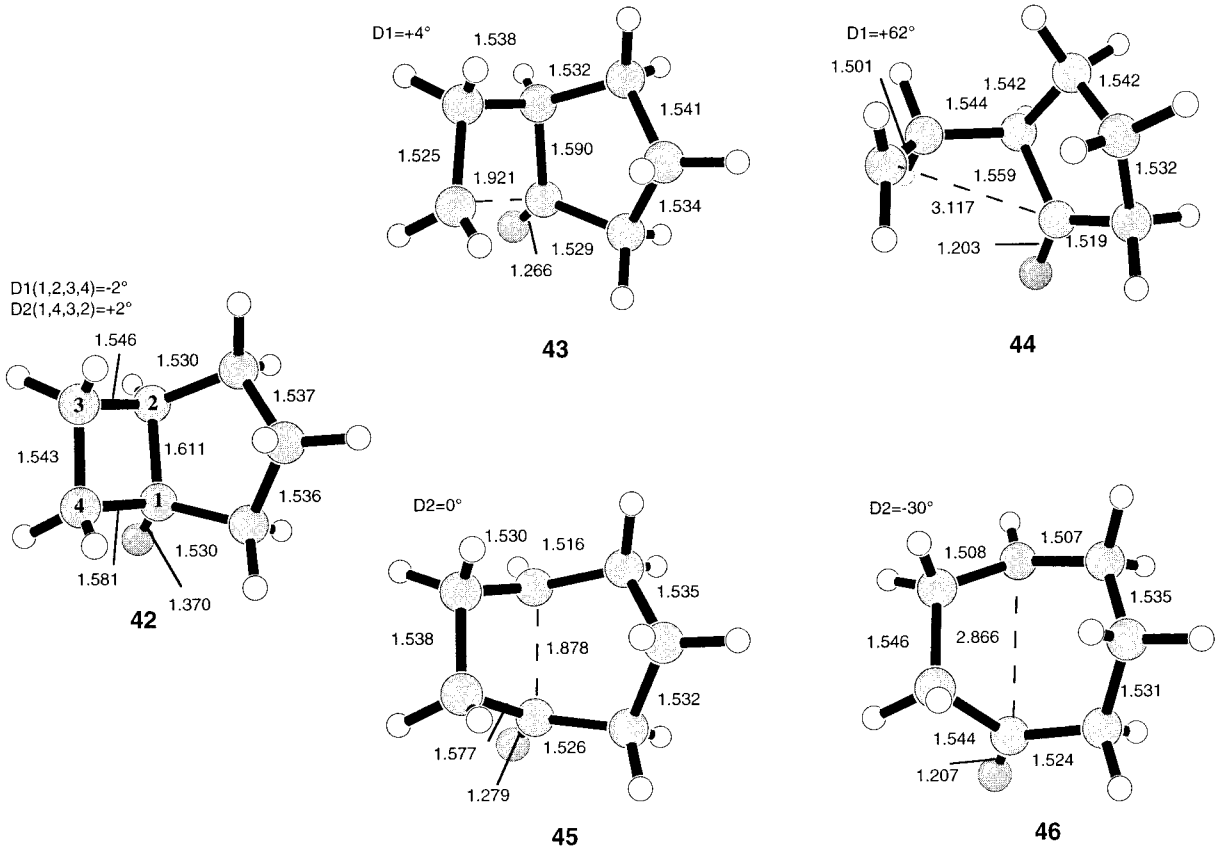

Figure 12. CASSCF/6-31G*-optimized bicycloheptoxy geometries—bicycloheptoxy radical (**42**), transition structures for bond **a** and bond **b** cleavage (**43** and **45**), and products of bond **a** and bond **b** cleavage (**44** and **46**).

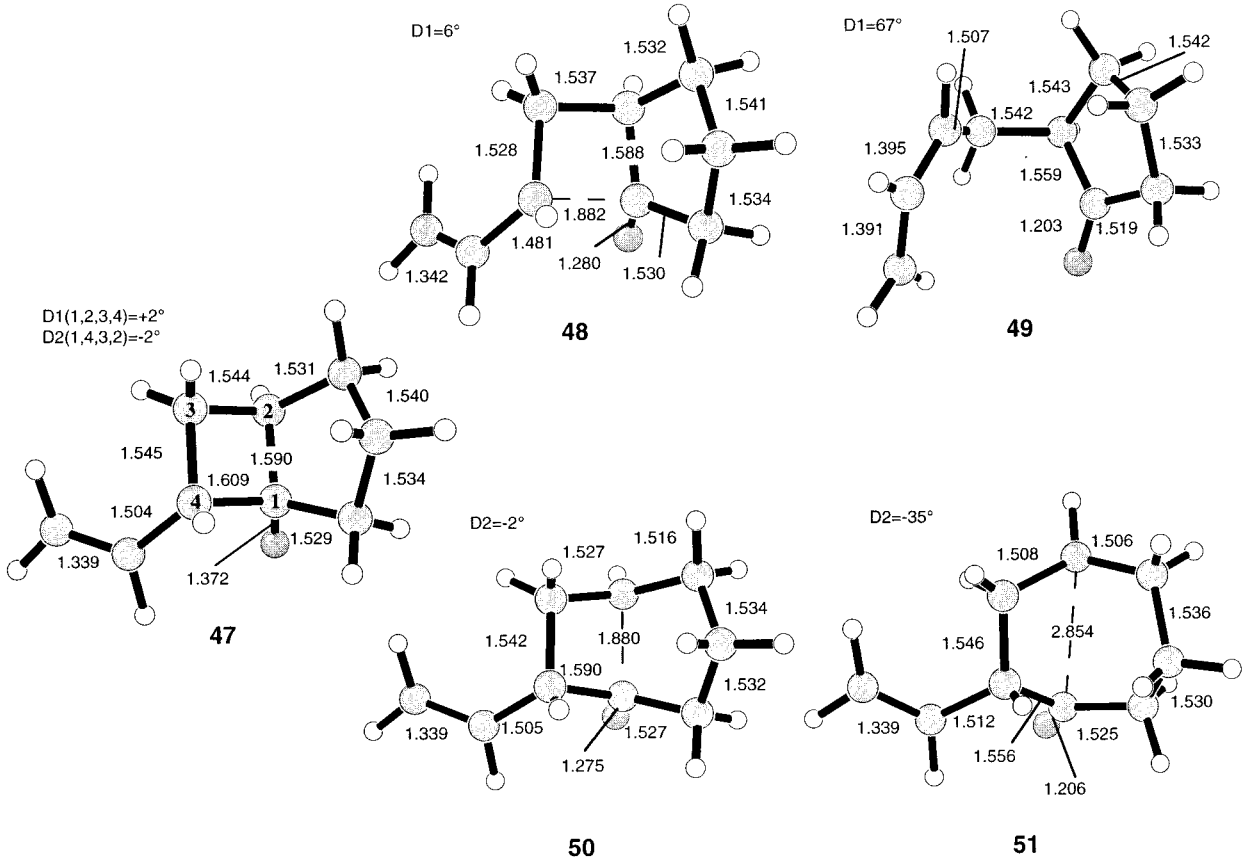

Figure 13. CASSCF/6-31G*-optimized vinylbicycloheptoxy geometries—vinylbicycloheptoxy radical (**47**), transition structures for bond **a** (allylic) and bond **b** cleavage (**48** and **50**), and products of bond **a** (allylic) cleavage and bond **b** cleavage (**49** and **51**).

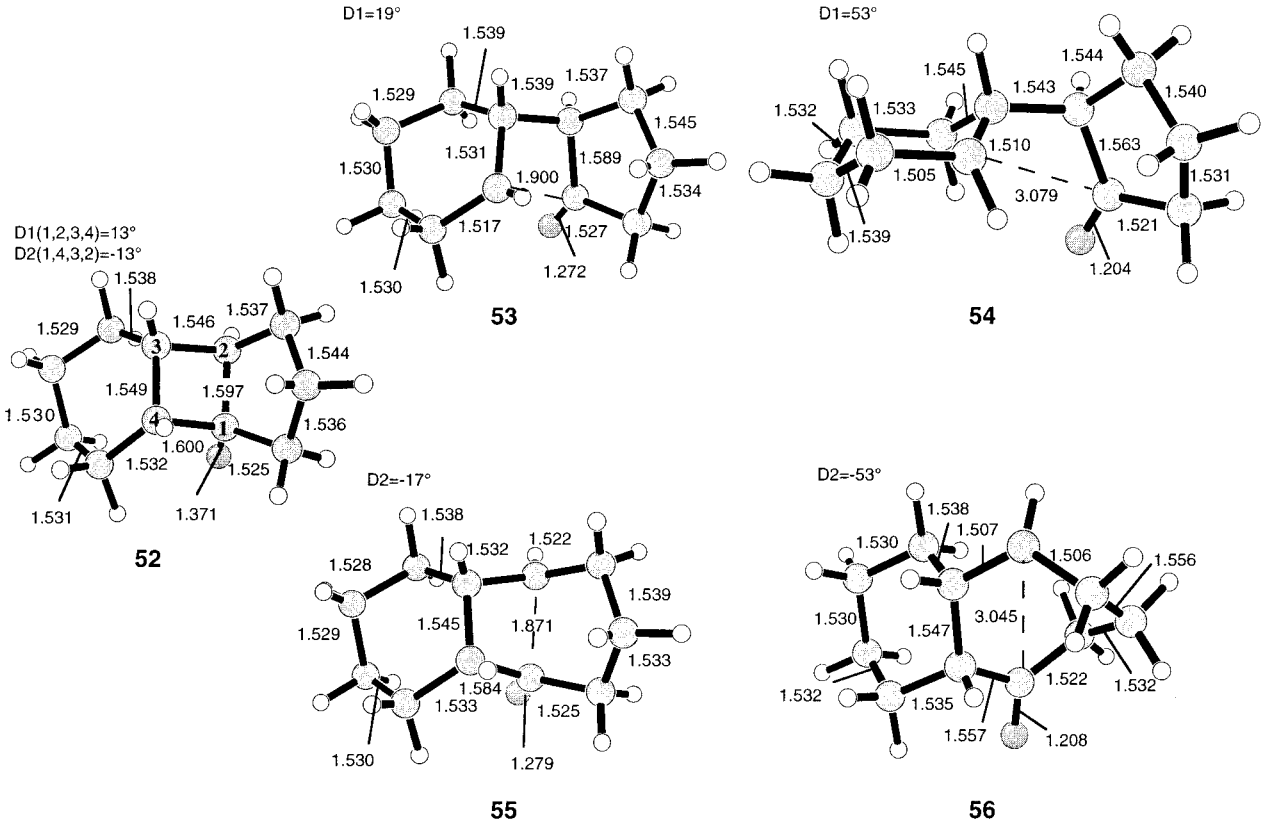

Figure 14. CASSCF/6-31G*-optimized tricycloundecoxy geometries—tricycloundecoxy radical (**52**), transition structures for bond **a** and bond **b** cleavage (**53** and **55**), and products of bond **a** and bond **b** cleavage (**54** and **56**).

however, deviate considerably from the line. The transition structures for cyclopropoxy and cyclopentoxy cleavage are more stable than expected from their energies of reaction, while the transition structures for cyclobutoxy and cyclohexoxy cleavage are less stable than expected. We have recently proposed an explanation for this effect on the basis of orbital interactions through bonds (OITB).[11] This is discussed in more detail in the next section.

The activation and reaction energies for the bicyclic and tricyclic systems are shown in Figures 5 and 6, respectively. Both bond **a** cleavage and bond **b** cleavage were examined in each case, and the energies obtained are illustrated in Figure 11. These are all tertiary radicals, and might be expected to lie close to the line of best fit for the tertiary radicals, which is shown in the graph as a solid line. However, significant deviations are also observed for these systems, which we discuss in more detail below.

Figure 12 shows the optimized structures for system **T**. In **42**, the oxygen is held pseudoaxial, so that pseudoequatorial cleavage cannot occur for either bond **a** or bond **b** cleavage. The lowest energy transition structure for bond **a** cleavage (**43**) has a CC−CC torsion angle of only 4°, which is small compared to that of the cyclobutoxy system **Q** (24°). Both the activation energy and the reaction energy are 2−3 kcal/mol more than for system **Q**. Bond **b** cleavage leading to **46** has an activation energy 4.6 kcal/mol lower than bond **a** cleavage, but it is only 0.9 kcal/mol more exothermic. As shown in Figure 11, the cleavage of bond **b** gives rise to a point that lies below the line of best fit for the tertiary radicals, while cleavage of bond **a** gives a point which lies on the line. Therefore, the simultaneous cleavage of the fused four- and five-membered rings leads to an anomalously low activation barrier, relative to cleavage of the four-membered ring alone.

Figure 13 shows the results for the vinyl-substituted system **U**. The product of allylic (bond **a**) cleavage (**49**) now lies 15 kcal/mol below that of bond **b** cleavage (**51**). Nevertheless, the transition structure for bond **b** cleavage still lies below that for bond **a** cleavage. The addition of the vinyl group lowers the barrier (**48**) for bond **a** cleavage by 3.6 kcal/mol, whereas the product has been stabilized by more than 4 times this amount (15.1 kcal/mol). Therefore, the allylic stabilization must develop relatively late along the reaction coordinate. The energies of the transition structure **50** and product **51** of bond **b** cleavage are similar to those in system **T**. In Figure 11, the point for bond **b** cleavage lies below the line of best fit for the tertiary radicals, very close to the point corresponding to bond **b** cleavage in system **T**, but the point corresponding to bond **a** cleavage to form the allyl radical lies significantly above the line.

The energies for the tricyclic systems **V** and **W** are shown in Figure 6. The major effect of adding the cyclohexane ring is to stabilize the transition structure for bond **a** cleavage (**53**) relative to that in system **T** by 2.8 kcal/mol, because the product **54** is now a secondary radical (Figure 14). There is virtually no change in either the activation barrier or the product stability for bond **b** cleavage. Therefore, the transition structure for cleavage of bond **b** (**55**) is still 2.3 kcal/mol below that for cleavage of bond **a**, even though the five-membered ring product **54** is now 1.2 kcal/mol *more* stable than the seven-

(11) Sawicka, D.; Wilsey, S.; Houk, K. N. *J. Am. Chem. Soc.* **1999**, *121*, 864.

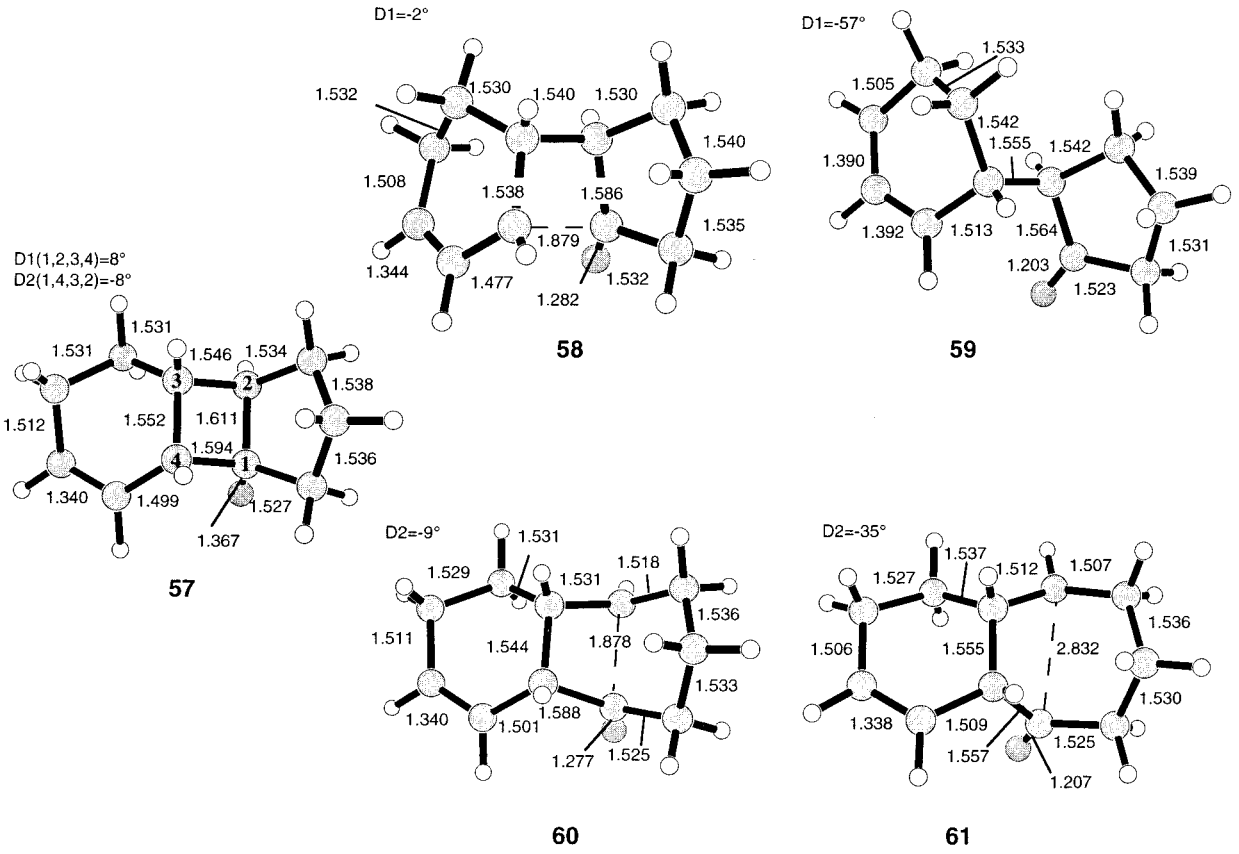

Figure 15. CASSCF/6-31G*-optimized tricycloundecenoxy geometries—tricycloundecenoxy radical (**57**), transition structures for bond **a** (allylic) and bond **b** cleavage (**58** and **60**), and products of bond **a** (allylic) and bond **b** cleavage (**59** and **61**).

Table 1. Energy Differences ($E_{TSa} - E_{TSb}$) between the Transition States for Bond a and Bond b Cleavage for Systems V1−V3 and W1−W3 at Different Levels of Theory

system	reactant	CASSCF/ 4-31G	CASSCF/ 6-31G*	UHF/ 6-31G*	UB3LYP/ 6-31G*
V	**52**	+2.9	+2.3	+2.6	+1.8
W	**57**	−0.1	+1.3	−0.2	+1.4[a]
V1	**62**	+3.2			
W1	**63**	+1.2			
V2	**64**	+3.3			
W2	**65**	+1.3			
V3	**66**	+2.9			
W3	**67**	−0.5			

[a] Transition structure for bond **a** cleavage optimized with a constrained C−C bond-breaking distance of 1.665 Å.

membered ring product **56**. As shown in Figure 11, bond **b** cleavage is relatively unaffected by the additional six-membered ring and lies close to the points corresponding to bond **b** cleavage in **T** and **U**. The point for bond **a** cleavage lies just below the line, close to that of system **T**.

Introduction of a double bond (system **W**) produces a large stabilizing effect on the radical formed by cleavage of bond **a** relative to system **V**; the allylic product **59** lies 11.8 kcal/mol below the secondary radical product **61** of bond **b** cleavage (Figure 15). The results obtained for this system are directly analogous to those obtained for system **U**. Once again, very little of the allylic stabilization is reflected in the energy of the transition state. The barrier for the allylic cleavage (**58**) lies 1.3 kcal/mol above the barrier for bond **b** cleavage (**60**), which is unchanged by the addition of the double bond. The double bond stabilizes the transition structure by only 0.6 kcal/mol. Returning to Figure 11, it is clear that the allylic cleavage is exceptionally difficult for a process leading to such a stabilized product; consequently, cleavage **b** is favored. In Figure 11, a more appropriate line of best fit might be that drawn through exocyclic (bond **a**) cleavage in the four systems **T**−**W** and cyclobutoxy; this is shown by the dashed line. This line has a slope of 0.18, which predicts that on average less than 20% of the product stabilization shows up in these systems. Both this line and the solid line appropriate for tertiary alkoxy radicals show that exocyclic cleavage of four-membered rings is disfavored relative to the simultaneous cleavage of four- and five-membered rings, even with allylic stabilization of the product.

To check our results, the transition structures for systems **V** and **W** were also reoptimized using UHF/6-31G* and UB3LYP/6-31G* techniques. In each case the barrier height for bond **a** cleavage is reduced on going from the saturated to the unsaturated system, but still remains either higher than or very close to the transition structure for bond **b** cleavage. For each method, only a small fraction of the allylic stabilization shows up in the transition state for bond **a** cleavage. The transition structure for bond **a** cleavage for the unsaturated system **V** could not be fully optimized at the UB3LYP/6-31G* level, as the surface is extremely flat along the bond-breaking coordinate. However, an estimate of the energy was obtained by taking a series of partial optimizations, constraining the cleaving bond each time. The optimum bond length was found to be around 1.665 Å, which is remarkably short for a breaking bond in a transition state. However, on optimizing the reactants for **V** and **W** at the UB3LYP/6-31G* level, it was found that bond

Scheme 3

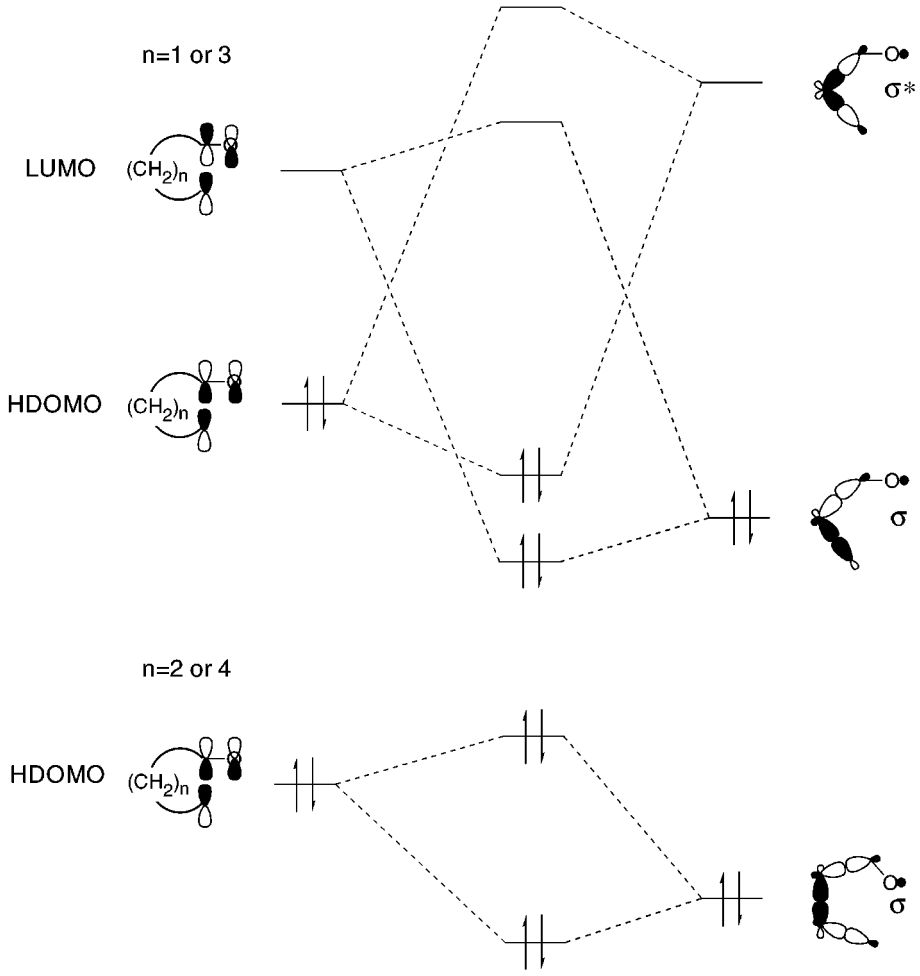

b was exceptionally long (1.71 Å) in both cases, indicating a strong predisposition to cleave bond **b** at this level of theory. In fact, the UB3LYP/6-31G*-computed barriers for bond **b** cleavage are only 0.2 and 0.1 kcal/mol in **V** and **W**, respectively. This predisposition is not observed in the UHF/6-31G*- or CASSCF/6-31G*-optimized reactants, which have barriers for bond **b** cleavage of around 8 and 5 kcal/mol, respectively.

Finally, to determine the effect of the methyl groups present in the experimental system, we computed the relative barrier heights in six other systems (**V1**−**V3**, **W1**−**W3**) (Scheme 2) at the 4-31G level. The results (Table 1) show that the effect of the methyl groups is significant. The methyl groups in the model systems **V1**, **W1**, **V2**, and **W2** were found to increase the energy difference between the transition structures in each case. The effect on the saturated systems **V1** and **V2** is small; the energy difference is increased by only 0.3 and 0.4 kcal/mol, respectively. However, for the enone systems **W1** and **W2**, the energy difference is increased by 1.3 and 1.4 kcal/mol, respectively. The methyl group in **W1** is expected to stabilize the transition state for bond **b** cleavage, while that in **W2** destabilizes the transition state for bond **a** cleavage. The methyl group in **V3** had no effect, while that in **W3** caused the energy of transition state **a** to drop another 0.4 kcal/mol below transition state **b**. The overall effect of the three methyl groups is estimated to increase the energy difference between the barriers by 0.7 kcal/mol for the saturated system to 3.6 kcal/mol at the CASSCF/4-31G//CASSCF/STO-3G level and to increase the energy difference by 2.3 kcal/mol in the unsaturated system to 2.2 kcal/mol.

Discussion

The calculations provide a good account of the experimentally observed direction of ring cleavage. In every case, there is a preference for cleavage of bond **b** to form the seven-membered ring, even in the unsaturated systems **U** and **W**, where bond **a** cleavage results in the formation of a significantly stabilized allyl radical. Two factors contribute to this regioselectivity: a lack of stabilization of the transition structures leading to allyl radicals, and anomalously low activation energies for bond **b** cleavage relative to exocyclic cleavage of a four-membered ring.

First, we address the question of why stabilization of the allylic products **49** and **59** is not felt in the transition structures **48** and **58** leading to them. This effect must be attributed to a lack of radical delocalization, which is also reflected in the significantly different C−C bond lengths of the allyl fragment (1.34 Å vs 1.48 Å) in the transition structures. In fact, the bond adjacent to the double bond changes by only 0.2 Å between the reactants and the transition structure, which is less than 20% of the change between the reactants and products (0.11 Å). The transition structures are early, as indicated by the short breaking C−C bond lengths (∼1.9 Å) in all cases. Therefore, the allylic stabilization must take effect later along the reaction coordinate.

Our calculations predict that the unsaturated allylic group will have a very small stabilizing kinetic effect, whereas the experimental results show the effect is slightly destabilizing. This does not appear to be a problem with the method used, as every method predicts a relative decrease in the seven-membered ring product. This is most probably related to the methyl substituents, which were found to stabilize the transition state for bond **b** cleavage in **W1**, and destabilize the transition state for bond **a** cleavage in **W2**.

The biggest surprise observed experimentally, which is well reproduced by our calculations, is the slow rate of exocyclic four-membered ring cleavage relative to the rate of cleavage in fused four- and five-membered rings. This preference is also observed in analogous cyclobutylcarbinyl compounds[13] and may be attributed to OITB, which have been proposed to disfavor cleavage in even-membered rings and favor cleavage in odd-membered rings.[14] The role of OITB, proposed first by Hoffmann, has been invoked to explain many spectroscopic phenomena.[15] Verhoeven pointed out how such interactions could influence transition states and interpreted some experimental data on this basis.[14] We find this to be a good explanation for the trends summarized in Figures 10 and 11. Scheme 3 shows a sketch of the relevant orbitals at the cleavage transition states. The diagrams on the left-hand side resemble the σ and σ^* orbitals of a breaking CC bond interacting with a p orbital of the oxygen. These interactions give rise to three orbitals: the highest doubly occupied molecular orbital (HDOMO), the lowest unoccupied molecular orbital (LUMO), and the singly occupied MO, or SOMO (not shown), which is still mainly on the alkoxy oxygen in these early transition states. The HDOMO and the LUMO interact with the orbitals of the σ framework, shown on the right-hand side of the diagram. For an odd-length polymethylene chain, such as $-(CH_2)_3-$, the highest σ orbital is an antibonding combination of CC bond orbitals. It is of the correct symmetry to interact strongly with the LUMO of the cleaving alkoxy radical. The lowest σ^* orbital of $-(CH_2)_3-$ is locally symmetric and will mix with and stabilize the transition state HDOMO. Such a reaction is said to be *σ-assisted*.[14] The symmetries of the highest σ and lowest σ^* orbitals of an even-length polymethylene fragment are reversed. The highest σ orbital will cause the HDOMO to be destabilized, while the lowest σ^* orbital only interacts with the LUMO (not shown). This type of reaction is referred to as *σ-resisted*.[14] The energy of the SOMO is not affected differentially by the σ framework, since there is almost no coefficient on the carbon atom attached to the oxygen in the transition state.

Finally, we return to substituent effects on the rates of cleavage shown in Figure 7. As reflected by the relatively flat lines (slopes ~0.2) in Figure 7b, alkyl substitution at the alkoxy carbon (which becomes the carbonyl carbon) influences the transition states much less than the products. Alkyl groups stabilize carbonyls by donating electron density into the π^* orbital of the carbonyl group. However, in the transition state for cleaving an alkoxy radical, the LUMO of the breaking bond, which eventually becomes the π^* orbital of the carbonyl, is high in energy such that this electron donation is small.

Alkyl substitution at the forming radical center has a larger effect in the transition state. The transition state and the radical product are both stabilized by electron donation into the SOMO; the energy of the SOMO does not change much on going from the transition state to the products. Much of the product radical stabilization (>50%) is felt in the transition state as indicated in Figure 7a, where the gradients of the lines are 0.56−0.79.

Conclusions

In this work we show that two factors contribute to the anomalous relative rates of ring-opening found by Zhang and Dowd: (1) the cleavage of cyclobutoxy radicals is slow relative to the simultaneous cleavage of four- and five-membered ring oxy radicals, due to stabilizing OITB from the five-membered ring, and (2) cleavage to form an allyl radical is unexpectedly slow as the transition state occurs early along the reaction coordinate, with the electron density still localized in the breaking C−C bond, not delocalized over the allyl fragment.

We have also expanded the observations made by Choo and Benson on relationships between activation energies and reacting energetics. We have demonstrated the dramatic difference in transition state stabilization depending on where the alkoxy radical is substituted. Methyl substitution at the forming radical center on the leaving group leads to large amounts of transition state stabilization, almost two-thirds of the product stabilization. Methyl substitution on the alkoxy carbon, on the other hand, leads to very small amounts of stabilization in the transition states (less than 20% of the product stabilization in most cases). These differences arise from the difference in orbital energies of the electron-donating methyl σ orbitals and the electron-accepting orbitals (SOMO or LUMO) in the breaking σ bond.

Acknowledgment. We are grateful to the National Science Foundation for financial support of this research and to the National Center for Supercomputing Applications, University of Illinois at Urbana-Champaign, and the UCLA Office of Academic Computing for computational resources. S.W. thanks the Royal Society for a NATO Fellowship and the Fulbright Commission for a scholarship.

Supporting Information Available: A table containing the absolute energies of all the critical points located in this work and the Cartesian coordinates for the corresponding points and two figures with cyclopropoxyl and cyclohexyl reaction geometries. This material is available free of charge via the Internet at http://pubs.acs.org.

JO990652+

(12) (a) Stirling, C. J. M. *Tetrahedron* **1985**, *41*, 1613. (b) Stirling, C. J. M. *Pure Appl. Chem.* **1984**, *56*, 1781. (c) Earl, H. A.; Marshall, D. R.; Stirling, C. J. M. *J. Chem. Soc., Perkin Trans. 2* **1983**, 779. (d) Earl, H. A.; Stirling, C. J. M. *J. Chem. Soc., Perkin Trans. 2* **1987**, 1273. (e) Bury, A.; Earl, H. A.; Stirling, C. J. M. *J. Chem. Soc., Perkin Trans. 2* **1987**, 1281. (f) Tonachini, G., Bernardi, F.; Schlegel, H. B.; Stirling, C. J. M. *J. Chem. Soc., Perkin Trans. 2* **1988**, 705.

(13) (a) Lange, G. L.; Gottardo, C. *J. Org. Chem.* **1995**, *60*, 2183. (b) Lange, G. L.; Merica, A.; Chimanikire, M. *Tetrahedron Lett.* **1997**, *38*, 6371. (c) Lange, G. L.; Gottardo, C. *J. Org. Chem.* **1994**, *35*, 8513.

(14) Verhoeven, J. W. *Recl. Trav. Chim. Pays-Bas* **1980**, *99* 375.

(15) (a) Hoffmann, R.; Imamura, A.; Hehre, W. *J. Am. Chem. Soc.* **1968**, *90*, 1499. (b) Paddon-Row: M. N.; Patney, H. K.; Brown, R. S.; Houk, K. N. *J. Am. Chem. Soc.* **1981**, *103*, 5575 and references therein.